HAL
archives-ouvertes.fr

Defects and strain enhancements of second-harmonic generation in Si/Ge superlattices

Matteo Bertocchi, E. Luppi, Elena Degoli, Valérie Véniard, Stefano Ossicini

▶ **To cite this version:**

HAL Id: hal-01024364

https://hal-polytechnique.archives-ouvertes.fr/hal-01024364

Submitted on 16 Jul 2014

Defects and strain enhancements of second-harmonic generation in Si/Ge superlattices

Matteo Bertocchi, Eleonora Luppi, Elena Degoli, Valérie Véniard, and Stefano Ossicini

Articles you may be interested in

Structural, dynamic, and vibrational properties during heat transfer in Si/Ge superlattices: A Car-Parrinello molecular dynamics study
J. Appl. Phys. **114**, 234905 (2013); 10.1063/1.4850935

Thermal conductivity in strain symmetrized Si/Ge superlattices on Si(111)
Appl. Phys. Lett. **83**, 4184 (2003); 10.1063/1.1628819

Second-harmonic generation from chemically modified Ge(111) interfaces
J. Chem. Phys. **116**, 6745 (2002); 10.1063/1.1454242

Defect-enhanced second-harmonic generation in (Si m Ge n) p superlattices
Appl. Phys. Lett. **72**, 2072 (1998); 10.1063/1.121279

Interfaces of strained layer (Ge n Si m) p superlattices studied by second-harmonic generation
J. Vac. Sci. Technol. B **15**, 1112 (1997); 10.1116/1.589423

Defects and strain enhancements of second-harmonic generation in Si/Ge superlattices

Matteo Bertocchi,[1] Eleonora Luppi,[2] Elena Degoli,[1,3] Valérie Véniard,[4] and Stefano Ossicini[3,5]

[1]*Dipartimento di Scienze e Metodi dell'Ingegneria, Università di Modena e Reggio Emilia, Via Amendola 2 Padiglione Morselli, I-42122 Reggio Emilia, Italy*
[2]*Laboratoire de Chimie Théorique, Université Pierre et Marie Curie, 75005 Paris, France*
[3]*Istituto di Nanoscienze-CNR-S3, Via Campi 213A, 41125 Modena, Italy*
[4]*Laboratoire des Solides Irradiés, Ecole Polytechnique, CNRS, CEA-DSM and European Theoretical Spectroscopy Facility (ETSF), Route de Saclay, 91128 Palaiseau, France*
[5]*Dipartimento di Scienze e Metodi dell'Ingegneria and Centro Interdipartimentale En&Tech, Università di Modena e Reggio Emilia, Via Amendola 2 Padiglione Morselli, I-42122 Reggio Emilia, Italy*

Starting from experimental findings and interface growth problems in Si/Ge superlattices, we have investigated through *ab initio* methods the concurrent and competitive behavior of strain and defects in the second-harmonic generation process. Interpreting the second-harmonic intensities as a function of the different nature and percentage of defects together with the strain induced at the interface between Si and Ge, we found a way to tune and enhance the second-harmonic generation response of these systems. © *2014 AIP Publishing LLC*. [http://dx.doi.org/10.1063/1.4880756]

Si/Ge superlattices (SLs) have important technological applications in the field of thermoelectricity,[1–3] spintronics,[4,5] and photonics devices.[6–13] Their linear optical-properties can be controlled and tuned by quantum confinement which revealed to be efficient for the electronic band-gap design, overcoming the poor recombination efficiency of indirect gap through zone folding.[5,14–16] This manipulation at the nanometer scale demonstrated that Si/Ge SLs are efficient light-emitting semiconductors.[6,7,10,13,17–20] Moreover, these systems have also a great potential in nonlinear optics for technological photonic applications and second-order optical response ($\chi^{(2)}$) studies have been carried on since the 1990s.[8,9,11,12,19–26] All these studies were mainly focused on optical second-harmonic generation (SHG) which has finally matured into a powerful technique for probing the electronic and structural properties of materials.[27–30] In fact, this nonlinear optical spectroscopy brought a significant progress in manipulating materials thanks to its sensitivity to defects, steps, strain, roughness, and chemical modification.[26]

Like bulk Si and Ge, Si_m/Ge_n SLs possess inversion symmetry for m or/and n even where m is the number of layers of Si while n is the number of layers of Ge. Consequently SHG is expected to be dipole-forbidden. However, theoretical calculations[12] are in contradiction with some experiments[8,22–24] where the measured signal for odd-periodicity material was found to be smaller than that theoretically expected, whereas the even-periodicity superlattices exhibited a SHG response comparable to the odd ones. This smaller intensity has been related to the nonuniformity of the superlattice layer thickness resulting during the growth process.[22–24] Indeed, in these works, it is suggested that the loss of an abrupt interface, originated during deposition from strain and monoatomic steps in the bulk-terminated Si(001) surface, creates defects and anti-phase domains that may di-minish the bulk dipole-allowed macroscopic SHG response.[22] These defects develop a mixture of even and odd number of layers[24] inside the structure. Moreover, the experimental results suggest that the SHG arises locally at the strained interface from the Si–Ge bonds.[8,24] From a theoretical point of view, Ghahramani, Moss, and Sipe[11,12] found that the dipolar SHG response from Si_n/Ge_n SLs is comparable to that of bulk materials, such as GaAs, which do not have inversion symmetry. Moreover, this response decreases with increasing n as it approaches the sum of contributions from series of separated interfacial regions (i.e., multiple quantum wells).

In this work, we demonstrate, fully *ab initio*, how to enhance second-harmonic generation in Si_m/Ge_n superlattices through the formation of defects and strain at the interface of Si and Ge. We analyze different types of defects[24] discussing the modulation that they induce on the SHG signal, bridging the gap between theoretical calculations and experimental measurements. All the ground state calculations have been performed using the *abinit* code.[31]

We first computed the SHG spectroscopy in Si_n/Ge_n (001) superlattices, studying how the second-order nonlinear response is modified by the thickness n of the two insulating slabs. We focused on systems with n = 3,4,5 as going above 5 layers of Ge induces the formation of structural defects in Si_m/Ge_n SLs which are not able to contain the strong compression of Ge.[8,24,32] To simulate these systems we used a supercell approach where our unit cell is tetragonal for the Si_4/Ge_4 (4 atoms of Si and 4 atoms of Ge) and triclinic for the Si_5/Ge_5 (5 atoms of Si and 5 atoms of Ge, $\alpha = \beta = 77.451°$) and Si_3/Ge_3 (3 atoms of Si and 3 atoms of Ge, $\alpha = \beta = 82.273°$). In Fig. 1 we show as example the Si_5/Ge_5 SL where Ge atoms are represented in violet and Si atoms in yellow. The atoms were also enumerated as we reported atomic/layer distances and angles for all the structures in Tables I–III.
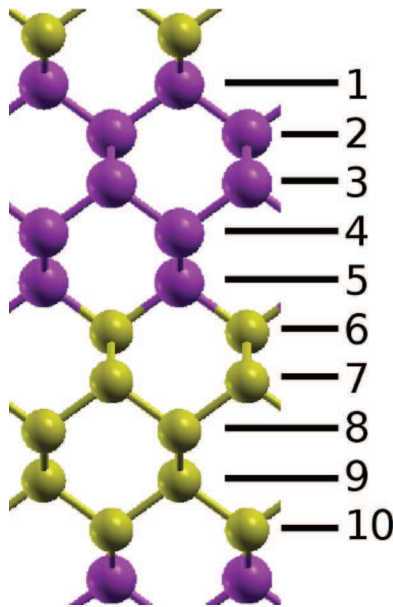
FIG. 1. The Si_5/Ge_5 SL is represented. The Ge atoms are represented with violet/dark-gray balls and Si atoms with yellow/light-gray balls. The atoms were enumerated in correspondence to Table I where the atomic/layer distances and angles are reported.

Moreover, to compare our outcomes with a realistic interface,[22,24] we impose the in-plane lattice parameter of the interface (i.e., along the (100) and (010) directions) to be equal to that of bulk Si: a_{Si} = 5.389 Å. This theoretical value calculated at 0 K well reproduces the experimental one:[33] a_{Si} = 5.430 Å at 6.4 K. In this way we obtained structures that correspond to Si_n/Ge_n superlattice grown on top of Si (001) perpendicularly to its surface. The lattice parameter along the (001) direction has been theoretically calculated as the one that minimizes the total energy of the system after a relaxation

TABLE I. Si_5/Ge_5 structures. The atomic enumeration starts from the top-most Ge atom (#1) and increases going down into the Ge slab, the interface Si atom (#6) and the Si slab. Layer distances correspond to the separation between the current and the underlying layer. Atomic distances correspond to the distance between the current and the underlying atom. The angle is calculated as the one formed by the bonds of the atom with the top and bottom atoms. In non-relaxed system (that has a diamond like structure) the distances and the angles are all equal.

Atoms	Layer distances (bohr)	Atomic distances (bohr)	Angles (deg)
Si_5/Ge_5 non-relaxed			
	2.625	4.452	110.3
Si_5/Ge_5 relaxed			
1(Ge)	2.718	4.507	110.8
2(Ge)	2.709	4.502	111.3
3(Ge)	2.709	4.502	111.2
4(Ge)	2.718	4.507	111.3
5(Ge)	2.624	4.451	110.8
6(Si)	2.533	4.398	109.8
7(Si)	2.543	4.404	109.4
8(Si)	2.543	4.404	109.5
9(Si)	2.533	4.398	109.4
10(Si)	2.624	4.451	109.8

TABLE II. Si_4/Ge_4 structures. The atomic enumeration starts from the top-most Ge atom (#1) and increases going down into the Ge slab, the interface Si atom (#5) and the Si slab. Layer distances correspond to the separation between the current and the underlying layer. Atomic distances correspond to the distance between the current and the underlying atom. The angle is calculated as the one formed by the bonds of the atom with the top and bottom atoms. In non-relaxed system (that has a diamond like structure) the distances and the angles are all equal.

Atoms	Layer distances (bohr)	Atomic distances (bohr)	Angles (deg)
Si_4/Ge_4 non-relaxed			
	2.625	4.452	110.3
Si_4/Ge_4 relaxed			
1(Ge)	2.714	4.505	110.8
2(Ge)	2.706	4.500	111.2
3(Ge)	2.721	4.509	111.3
4(Ge)	2.631	4.556	110.9
5(Si)	2.536	4.400	109.9
6(Si)	2.546	4.405	109.5
7(Si)	2.530	4.396	109.4
8(Si)	2.616	4.447	109.8

of the atomic positions; its value is 8.33, 11.11, and 13.89 Å for the n = 3,4,5 systems, respectively.

In order to discuss the origin of SHG signal, we have considered two classes of systems: (i) the ideal non-relaxed SLs, where the atomic configuration of the bulk is perfectly preserved and (ii) the Si/Ge strained SLs obtained through relaxation of the ideal atomic positions in the cell.

The structural differences between the non-relaxed SLs and the relaxed SLs are reported for Si_5/Ge_5 in Table I, for Si_4/Ge_4 in Table II, and for Si_3/Ge_3 in Table III. In Table I the atomic enumeration starts from the topmost Ge atom (#1) and increases going down into the Ge slab, the interface Si atom (#6) and the Si slab (see Fig. 1). Layer distances correspond to the separation between the current and the underlying layer. Atomic distances correspond to the distance between the

TABLE III. Si_3/Ge_3 structures. The atomic enumeration starts from the top-most Ge atom (#1) and increases going down into the Ge slab, the interface Si atom (#4) and the Si slab. Layer distances correspond to the separation between the current and the underlying layer. Atomic distances correspond to the distance between the current and the underlying atom. The angle is calculated as the one formed by the bonds of the atom with the top and bottom atoms. In non-relaxed system (that has a diamond like structure) the distances and the angles are all equal.

Atoms	Layer distances (bohr)	Atomic distances (bohr)	Angles (deg)
Si_3/Ge_3 non-relaxed			
	2.625	4.452	110.3
Si_3/Ge_3 relaxed			
1(Ge)	2.714	4.505	110.8
2(Ge)	2.714	4.505	111.3
3(Ge)	2.625	4.452	110.8
4(Si)	2.536	4.400	109.9
5(Si)	2.536	4.400	109.4
6(Si)	2.625	4.452	109.9

current and the underlying atom. The angle is calculated as the one formed by the bonds of the atom with the top and bottom atoms. In non-relaxed system (that has a diamond like structure) the distances and the angles are all equal. The same is reported for Si_4/Ge_4 in Table II except that for this system the atomic enumeration starts from the topmost Ge atom (#1) and increases going down into the Ge slab, the interface Si atom (#5) and the Si slab and for Si_3/Ge_3 in Table III where in this case the atomic enumeration starts from the topmost Ge atom (#1) and increases going down into the Ge slab, the interface Si atom (#4) and the Si slab.

We calculated $\chi^{(2)}_{xyz}$ and $\chi^{(2)}_{zxy}$ using the *2light* code[34] where our nonlinear Time-Dependent Density Functional Theory (TDDFT) formalism is implemented.[34,35] We analyzed the second-order response in the independent particle approximation (IPA) and including the crystal local fields and excitonic effects. The crystal local fields[36] give a negligible contribution with respect to IPA at the frequencies of interest (the region where we compare with the experiments, i.e., below 2 eV). In particular, for homogeneous defect-free systems their effects are below 5% of the IPA-SHG signal, whereas for the non-uniform defect materials they remain around 5% up to 2.5 eV and become larger (20%) around 3.5 eV. We also investigated the excitonic effects through the α-kernel.[36–38] This kernel is a model static long-range kernel for TDDFT on top of a GW[39,40] or a scissor correction.[41] It relies on parameter α which is proportional to the inverse of the static dielectric constant of the material considered.[38] For each of the systems studied we calculated α taking the average of its static dielectric constant calculated along the x, y, and z directions. All the SHG spectra are enhanced by 30% with respect to the IPA ones but their shape is not modified. The same behavior has been observed for other type of materials.[36] This kernel is at the moment the most sophisticated way we have to simulate excitonic effects within our formalism and it has shown to be efficient to describe continuum excitons in semiconductor materials such as Si and Ge.[36,38] However, the Si_n/Ge_n SLs are more complex materials and we expect that the way we choose the parameter α and the static limit are too crude approximations. For these reasons and for the main scope of this article, which relies on a comparison between different systems, we reported the results in the IPA, as the inclusion of the excitonic effects does not cause any rearrangement of the peaks.

For the IPA calculations the main parameters to be converged are the reciprocal-lattice points (k) that sample the Brillouin Zone, the total number of occupied and unoccupied bands (b) to be considered in the process and the number of plane waves (pw). The convergency values depend on the particular system (size, relaxation, and type of defects). In the present calculations we have adopted sampling grids of random k-points composed by 6000 up to 18 000 points, b ranges between 50 and 300 whereas pw has been chosen between 1000 and 5000.

To compare our converged theoretical SHG spectra with experiments we have applied a scissor operator correction Δ to the LDA gap.[36,42] This scissor has been taken as the GW correction at the Γ point between the last valence (HOMO) and first conduction (LUMO) state. This HOMO-LUMO gap
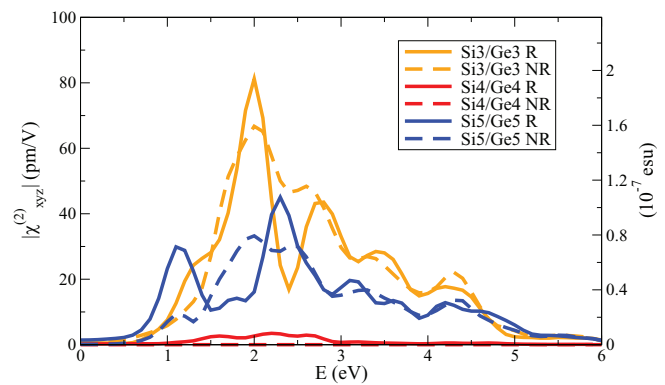

FIG. 2. Comparison of the SHG-IPA spectra for the Si_3/Ge_3 (orange/light gray lines), Si_4/Ge_4 (red/gray lines), Si_5/Ge_5 (blue/dark gray lines) systems. The SHG response of the relaxed (R) structures (continuous lines) is compared with that of the non-relaxed (NR) ones (dashed lines).

corresponds to the SLs gap, that becomes direct at Γ because of zone folding.[15,16] Δ depends on the thickness of the insulating slabs, being different for each system; the corrected *quasi-particle* energy gaps for $n = 3,4,5$ are 1.10, 0.97, 0.85 eV, respectively.

The results of the computed SHG spectra are reported in Fig. 2.

Looking at the non-relaxed systems, the theoretical predictions are confirmed. A vanishing signal is observed in the even Si_4/Ge_4 SL while SHG intensities of the same order of magnitude to those reported by Ghahramani *et al.*[12] are found for $n = 3,5$. We also obtained a good agreement concerning the shape of the spectra. The small differences arise from the band structures which was evaluated by using different theoretical approaches. It is also worth to notice that in accord to Ghahramani *et al.*[12] increasing n has the consequence to decrease the overall SHG intensity.

A different behavior is reported instead for relaxed superlattices. Odd Si_3/Ge_3 and Si_5/Ge_5 SLs related line shapes are modified depending on the internal strain of the structure. Si_3/Ge_3 exhibits a small enhancement of the response and a split of the resonance peaks both becoming greater in the Si_5/Ge_5 SL in particular around 1.16 eV (i.e., the resonance peak of the Si–Ge bond[24,43]) because of the greater internal strain; the calculated $\chi^{(2)}_{zxy}$ intensity at 1.16 eV (1064 nm) (14.5 pm/V $\simeq 3.5 \times 10^{-8}$ esu) is close to the experimental measurement (1.0×10^{-8} esu) of Xiao *et al.*[24] within a better agreement with respect to previous calculations[43] (8.5×10^{-8} esu). Moreover, a small non-vanishing signal is also observed for even Si_4/Ge_4 SL arising from the symmetry broken region at the interface. This is clear evidence of the role of the strain in centrosymmetric bulk materials.[44] In fact, from experimental observation[24] Si-on-Ge and Ge-on-Si interfaces can differ because of the different strain of Ge and Si top layers during MBE deposition. In order to take into account these effects, we have then relaxed the structure non-imposing the conservation of the initial (diamond-like) symmetry. It results in a difference between the top and bottom Si-Ge distances of the order of 0.02 bohr along the (001) direction. This difference is at the origin of an energetically more favorable configuration (with respect to the centrosymmetric relaxed
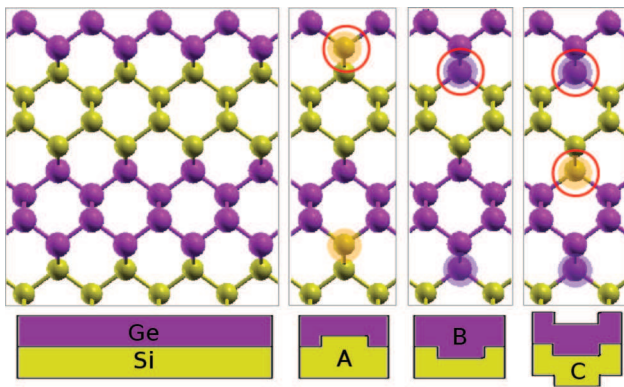
FIG. 3. Si_4/Ge_4 structure. On the left the defect-free crystalline system is reported (Si is represented by yellow/light gray atoms and Ge by violet/dark gray atoms). On the right the type A, type B, and type C defects are shown, the circle identify the modified atoms. On the bottom a schematic representation of the defect is proposed.

structure) and of the breaking of the inversion symmetry. However, it is worth to notice that Si_4/Ge_4 signal still remains more than one order of magnitude smaller than that of odd-periodicity materials around 1.16 eV (i.e., the frequency of experimental measurements), whereas experimentally they have been found to be of the same magnitude.[22–24] As a consequence, strain originating from the lattice mismatch alone cannot account for the experimental results and it becomes mandatory to handle the other possible source of the SHG signal, i.e., the structural defects.

For this reason, in the present work we have studied the defects originating from the non-uniform layering of the Si/Ge SL, as claimed in the experimental observations.[22–24,32] Thus it is important to understand which is their contribution to the global response, decoupling them from relaxation effects.

Therefore, we have studied different types of defects, in non-relaxed structure, and we have observed their influence comparing the related results with that of the defect-free Si_n/Ge_n SLs. In particular, according to the experimental evidence[24,32] we have addressed two roughness defects: *substitutional* and *ripple*, as shown in Fig. 3. In the *substitutional* case, a Ge atom at the interface is substituted by a Si atom (type A defect) or vice versa (type B) varying the slabs thickness; in the *ripple* one, heights are preserved but locally down-shifted by one layer (type C defect). Whereas type A and type B defects introduce different parity regions inside the material, defects of type C maintain the parity of the system. Other possible defects can be obtained as a combination of the *substitutional* and *ripple* ones. Therefore, once isolated the effect of these two basic defects on the SHG process, it is possible to deduce the total contribution due to any combination of them in a sort of additive mechanism.

The *substitutional* and *ripple* defects have been created in the Si_3/Ge_3, Si_4/Ge_4, and Si_5/Ge_5 SLs, observing their influence on the SHG response.

In Fig. 4 a detailed study of the type A, B, and C defects on the SHG signal is shown by varying the defect percentage inside the Si_4/Ge_4 superlattice. Comparing the spectra with the Si_4/Ge_4 (defect free) and Si_5/Ge_3 (i.e., the superlattice with 100% of type A defects) demonstrates a direct proportionality between the defect A percentage and the signal intensity. The same observations can be made for type B defects too (here one creates odd Si_3/Ge_5 regions). The general trend is then an increase of the Si_4/Ge_4 SHG signal due to the insertion of a non-vanishing odd component into the material. The proportionality seems to be more enhanced in A then in B and finally in C defects. However, it is worth to notice that beside this enhancement the SHG signal seems to be almost independent of the defect distribution (A, B, or C) inside the simulation cell. This proportionality has been observed also starting from odd-periodicity SLs, i.e., introducing type A defects inside the Si_5/Ge_5 structure. In this case the intensity is diminished as consequence of the introduction of an even periodicity region (i.e., Si_6/Ge_4).
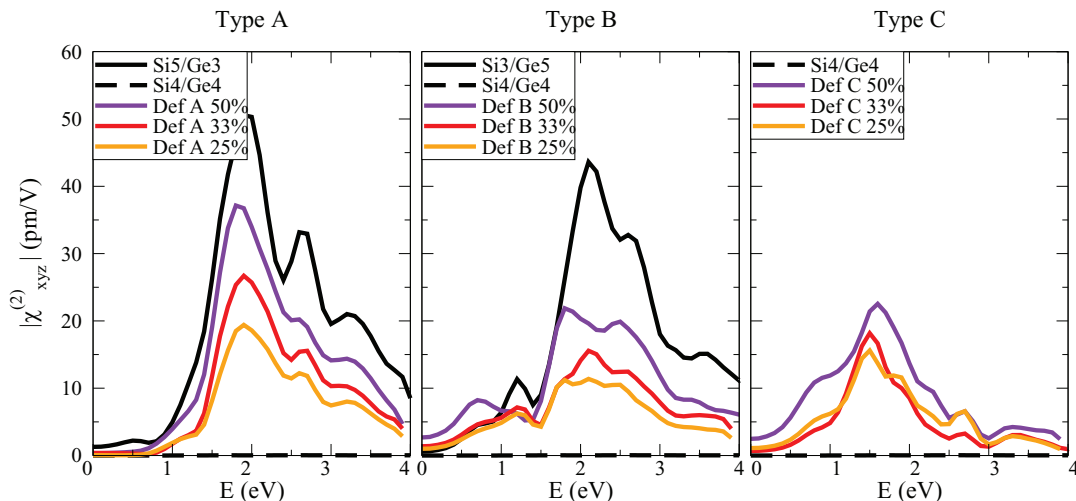

FIG. 4. Left: Comparison between the SHG-IPA spectra of the Si_4/Ge_4 non-relaxed system (black dashed line) with different percentages of type A defect (color/gray-scale lines) and that of the defect-free Si_5/Ge_3 (black continuous line). Center: Comparison between the SHG-IPA spectra of the Si_4/Ge_4 non-relaxed system (black dashed line) with different percentages of type B defect (color/gray-scale lines) and that of the defect-free Si_3/Ge_5 (black continuous line). Right: Comparison between the SHG-IPA spectra for type C defect with different concentration percentages (color/gray-scale lines) introduced in the Si_4/Ge_4 non-relaxed system (black dashed line).

Thus in Si_n/Ge_n SLs the nonlinear response is directly related to their periodicity: changing the periodicity defects can either increase the SHG process into even-superlattices or diminish the signal in odd-periodicity ones. Consequently the non-relaxed signal is mainly an additive combination of the single even/odd regions.

Defects of type C (Fig. 4 right panel) behave quite differently. Indeed, they do not introduce even/odd regions inside the material and therefore the intensity of the generated SHG signal is not linear with the percentage of defects. The intensity is still comparable with the one of the substitutional defects. Hence, as the substitutional ones, also non-planar deposition is an important source of SHG in the measured systems. Again, the same calculation performed on Si_5/Ge_5 structure shows that, modifying the periodicity, the defect decreases the total SHG intensity.

Similar results and trends have been observed for the $\chi^{(2)}_{zxy}$ component.

To be able to fully compare our results with the experiments, we have also relaxed our Si_4/Ge_4 system with 25% type B or type C defects and have compared the calculated SHG response with that of other cases: the unrelaxed Si_4/Ge_4 SL with the same amount of defects and the relaxed Si_4/Ge_4 and Si_5/Ge_5 defect-free system. Thus it is possible to access separately the role of defects and the role of relaxation. The results show that the relaxation at the interface with defects highly increases the SHG response (Fig. 5). This behavior is due to the higher distortion of the Si–Ge bonds in the defect systems. The same trend has been observed also for the odd SLs. Indeed all the nonlinear spectra related to the defected relaxed Si_4/Ge_4 SLs (defects concentration at 25%) are comparable with that of the without-defect Si_5/Ge_5 structure (black line) as experimentally observed. This indicates that the relaxation at the interface of Si and Ge alone does not account for the second-harmonic process in even-periodicity superlattices, and that also defects are responsible for the observed intensity. Instead, in without-defect odd-periodicity materials the relaxation at the interface modifies the final response, enhancing the SHG signal in more reconstructed structures (i.e.,
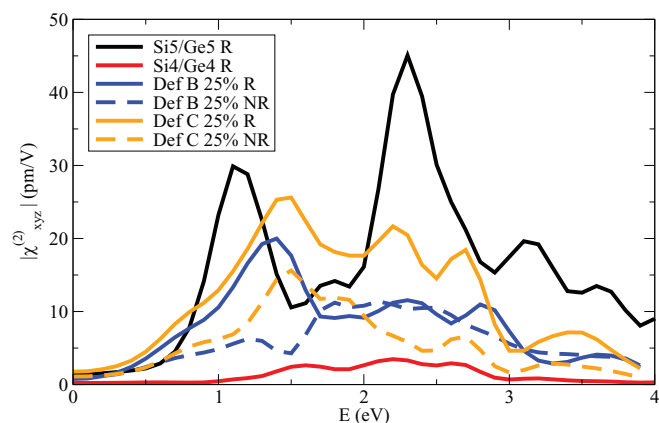
with greater n,[8,25] see Fig. 2). On the contrary, the presence of interface roughness (i.e., defects) in odd SLs reduces the final signal, as observed in our calculations.

In particular, this defect effect explains the experimental measurements of intensities similar in both even and odd short-period strained SLs, where the observed irregular thickness[8,22–24] is responsible for the increase (even) and decrease (odd) of the respective SHG signals. This ultimately level out the absolute intensities of the different periodicities.

In conclusion, we have demonstrated how to enhance and tune second-harmonic generation in odd/even Si_m/Ge_n superlattices analysing the competitive/concurrent influence of strain and defects. We were able to disentangle their single contribution in the SHG signal. Moreover, concerning defects, we were also capable to sample and discuss the possible defects through the combination of the two most fundamental: *substitutional* and *ripple*. In this way, we demonstrated the role of strain in generating and enhancing the SH signal in dipole-forbidden materials,[44] whereas it does not represent the major source of the nonlinear process, which is mainly determined by the Si/Ge interface roughness. We have further investigated the role of *substitutional* defects, which enhance the SHG in even-SLs and diminish it in odd-ones. A direct proportionality has been found to exist between the defect percentage and the SHG signal. It is then possible to control and tune the nonlinear response of a Si_n/Ge_n film by just varying their ratio inside the material. Moreover, *ripple* defects induce a comparable effect on the SH signal with respect to *substitutional* ones, but with a softer dependency on the defects percentage. Through a local control of the deposition thickness it could then be possible to design emitting films/flat devices with the desired nonlinear optical properties. These are really promising results also in view of recent achievements in Si/Ge deposition and nanostructuring techniques.[45]

FIG. 5. Comparison of the type B (blue) and type C (orange) defects Si_4/Ge_4 SHG-IPA response between the relaxed (R, continuous lines) and non-relaxed (NR, dashed lines) systems. The atomic bond strain induced by relaxation increases the system SHG signal. The nonlinear response of the relaxed Si_4/Ge_4 (red line) and Si_5/Ge_5 (black line) structures are shown for comparison.

[1]S.-M. Lee, D. G. Cahill, and R. Venkatasubramanian, Appl. Phys. Lett. **70**, 2957 (1997).

[2]M. L. Lee and R. Venkatasubramanian, Appl. Phys. Lett. **92**, 053112 (2008).

[3]J. Alvarez-Quintana, X. Alvarez, J. Rodriguez-Viejo, D. Jou, P. D. Lacharmoise, A. Bernardi, A. R. Goñi, and M. I. Alonso, Appl. Phys. Lett. **93**, 013112 (2008).

[4]F. Pezzoli, F. Bottegoni, D. Trivedi, F. Ciccacci, A. Giorgioni, P. Li, S. Cecchi, E. Grilli, Y. Song, M. Guzzi, H. Dery, and G. Isella, Phys. Rev. Lett. **108**, 156603 (2012).

[5]A. Giorgioni, F. Pezzoli, E. Gatti, S. Cecchi, C. K. Inoki, C. Deneke, E. Grilli, G. Isella, and M. Guzzi, Appl. Phys. Lett. **102**, 012408 (2013).

[6]M. Virgilio, G. Pizzi, and G. Grosso, J. Appl. Phys. **110**, 083105 (2011).

[7]G. Erley, R. Butz, and W. Daum, Phys. Rev. B **59**, 2915 (1999).

[8]C. Zhang, X. Xiao, N. Wang, K. K. Fung, M. M. T. Loy, Z. Chen, and J. Zhou, Appl. Phys. Lett. **72**, 2072 (1998).

[9]G. Mizutani, Y. Sonoda, S. Ushioda, T. Maeda, and J. Murota, Jpn. J. Appl. Phys. **34**, L119 (1995).

[10]U. Menczigar, G. Abstreiter, J. Olajos, H. Grimmeiss, H. Kibbel, H. Presting, and E. Kasper, Phys. Rev. B **47**, 4099 (1993).

[11]E. Ghahramani and J. E. Sipe, Appl. Phys. Lett. **62**, 2245 (1993).

[12]E. Ghahramani, D. J. Moss, and J. E. Sipe, Phys. Rev. Lett. **64**, 2815 (1990).

[13]D. Paul, Laser Photon. Rev. **4**, 610 (2010).

[14]M. d'Avezac, J.-W. Luo, T. Chanier, and A. Zunger, Phys. Rev. Lett. **108**, 027401 (2012).

[15] U. Gnutzmann and K. Clausecker, Appl. Phys. **3**, 9 (1974).

[16] M. E. Lazzouni and L. J. Sham, Appl. Phys. Lett. **63**, 3253 (1993).

[17] E. Ghahramani, D. J. Moss, and J. E. Sipe, Phys. Rev. B **41**, 5112 (1990).

[18] U. Schmid, N. E. Christensen, M. Alouani, and M. Cardona, Phys. Rev. B **43**, 14597 (1991).

[19] Y.-C. Chang, A. E. Chiou, and M. Khoshnevissan, J. Appl. Phys. **71**, 1349 (1992).

[20] H. M. Polatoglou, G. Theodorou, and C. Tserbak, Phys. Rev. B **49**, 8132 (1994).

[21] W. G. Aulbur, Z. H. Levine, J. W. Wilkins, and D. C. Allan, Phys. Rev. B **51**, 10691 (1995).

[22] D. J. Bottomley, G. Lüpke, M. L. Ledgerwood, X. Q. Zhou, and H. M. van Driel, Appl. Phys. Lett. **63**, 2324 (1993).

[23] D. J. Bottomley, J.-M. Baribeau, and H. M. van Driel, Phys. Rev. B **50**, 8564 (1994).

[24] X. Xiao, C. Zhang, A. B. Fedotov, Z. Chen, and M. M. T. Loy, J. Vac. Sci. Technol. B **15**, 1112 (1997).

[25] X. Zhang, X. Chen, L. Xuan, C. Peng, S. Pan, and G. Yang, Appl. Phys. Lett. **71**, 3359 (1997).

[26] G. Lüpke, Surf. Sci. Rep. **35**, 75 (1999).

[27] Y. Hirata, M. Nakajima, Y. Nomura, H. Tajima, Y. Matsushita, K. Asoh, Y. Kiuchi, A. G. Eguiluz, R. Arita, T. Suemoto, and K. Ohgushi, Phys. Rev. Lett. **110**, 187402 (2013).

[28] S. G. Rodrigo, H. Harutyunyan, and L. Novotny, Phys. Rev. Lett. **110**, 177405 (2013).

[29] A. M. Pugachev, V. I. Kovalevskii, N. V. Surovtsev, S. Kojima, S. A. Prosandeev, I. P. Raevski, and S. I. Raevskaya, Phys. Rev. Lett. **108**, 247601 (2012).

[30] D. Hsieh, J. W. McIver, D. H. Torchinsky, D. R. Gardner, Y. S. Lee, and N. Gedik, Phys. Rev. Lett. **106**, 057401 (2011).

[31] X. Gonze, B. Amadon, P.-M. Anglade, J.-M. Beuken, F. Bottin, P. Boulanger, F. Bruneval, D. Caliste, R. Caracas, M. Cote, T. Deutsch, L. Genovese, P. Ghosez, M. Giantomassi, S. Goedecker, D. Hamann, P. Hermet, F. Jollet, G. Jomard, S. Leroux, M. Mancini, S. Mazevet, M. J. T. Oliveira, G. Onida, Y. Pouillon, T. Rangel, G.-M. Rignanese, D. Sangalli, R. Shaltaf, M. Torrent, M. J. Verstraete, G. Zerah, and J. Zwanziger, Comput. Phys. Commun. **180**, 2582 (2009); X. Gonze, G.-M. Rignanese, M. Verstraete, J.-M. Beuken, Y. Pouillon, R. Caracas, F. Jollet, M. Torrent, G. Zerah, M. Mikami, P. Ghosez, M. Veithen, J.-Y. Raty, V. Olevano, F. Bruneval, L. Reining, R. Godby, G. Onida, D. R. Hamann, and D. Allan, Zeit. Kristallogr. **220**, 558 (2005).

[32] H. Matsuhata, K. Miki, K. Sakamoto, T. Sakamoto, and S. Yoshida, Phys. Rev. B **47**, 10474 (1993).

[33] D. N. Batchelder and R. O. Simmons, J. Chem. Phys. **41**, 2324 (1964).

[34] E. Luppi, H. Hübener, and V. Véniard, J. Chem. Phys. **132**, 241104 (2010).

[35] M. Bertocchi, E. Luppi, E. Degoli, V. Véniard, and S. Ossicini, Phys. Rev. B **86**, 035309 (2012).

[36] E. Luppi, H. Hübener, and V. Véniard, Phys. Rev. B **82**, 235201 (2010).

[37] L. Reining, V. Olevano, A. Rubio, and G. Onida, Phys. Rev. Lett. **88**, 066404 (2002).

[38] S. Botti, F. Sottile, N. Vast, V. Olevano, L. Reining, H.-C. Weissker, A. Rubio, G. Onida, R. D. Sole, and R. W. Godby, Phys. Rev. B **69**, 155112 (2004).

[39] L. Hedin, Phys. Rev. **139**, A796 (1965).

[40] G. Onida, L. Reining, and A. Rubio, Rev. Mod. Phys. **74**, 601 (2002).

[41] F. Nastos, B. Olejnik, K. Schwarz, and J. E. Sipe, Phys. Rev. B **72**, 045223 (2005).

[42] J. L. Cabellos, B. S. Mendoza, M. A. Escobar, F. Nastos, and J. E. Sipe, Phys. Rev. B **80**, 155205 (2009).

[43] E. Ghahramani, D. J. Moss, and J. E. Sipe, Phys. Rev. B **43**, 8990 (1991).

[44] M. Cazzanelli, F. Bianco, E. Borga, G. Pucker, M. Ghulinyan, E. Degoli, E. Luppi, V. Véniard, S. Ossicini, D. Modotto, S. Wabnitz, R. Pierobon, and L. Pavesi, Nat. Mater. **11**, 148 (2012).

[45] N. Geyer, Z. Huang, B. Fuhrmann, S. Grimm, M. Reiche, T.-K. Nguyen-Duc, J. de Boor, H. S. Leipner, P. Werner, and U. Gösele, Nano Lett. **9**, 3106 (2009).